An electron paramagnetic resonance study of a Cu^{2+}-doped guanidinium aluminium sulphate hexahydrate single crystal in the 3.9-433 K temperature range: Jahn-Teller effect

An electron paramagnetic resonance study of a Cu^{2+}-doped guanidinium aluminium sulphate hexahydrate single crystal in the 3.9–433 K temperature range: Jahn–Teller effect

Sushil K Misra, Yongmao Chang and Jerzy Kotlinski

Physics Department, Concordia University, 1455 de Maisonneuve Boulevard West, Montreal, Quebec H3G 1M8, Canada

Abstract. Detailed X-band (about 9.5 GHz) EPR studies on a Cu^{2+}-doped $C(NH_2)_3Al(SO_4)_2 \cdot 6H_2O$ single crystal have been carried out in the extended temperature range 3.9–433 K. Two magnetically inequivalent groups of Cu^{2+} complexes, each group consisting of three physically equivalent Cu^{2+} ions, were observed. The principal values of the $\mathbf{g}$- and $\mathbf{A}$-matrices characterizing the Cu^{2+} ion for one of these groups (site II) have been estimated at various temperatures, indicating a tetragonally elongated distortion of the octahedral local symmetry around the Cu^{2+} ions. The occurrences of static and dynamic Jahn–Teller effects below and above 423 K, respectively, have been observed.

1. Introduction

Guanidinium aluminium sulphate hexahydrate (GASH) $(C(NH_2)_3Al(SO_4)_2 \cdot 6H_2O)$ is a ferroelectric crystal [1, 2]. Electron paramagnetic resonance (EPR) studies on a GASH host crystal doped with the transition-metal ions Cr^{3+} [3–5], Fe^{3+} [6, 7], V^{3+} [4], Ti^{3+} [4], Mn^{3+} [4], VO^{2+} [4] and Mn^{2+} [8] have been reported. These studies revealed the existence of two physically equivalent but magnetically inequivalent Al^{3+} sites substituted by transition-metal ions, the local site symmetry at the Al^{3+} ion being trigonal.

As for the Cu^{2+} ion, room-temperature (RT) EPR studies on Cu^{2+} complexes in GASH were reported by Sczaniecki [9] for the orientation of the Zeeman field in two ($Z–Y$ and $X–Y$) magnetic panes. The natures of the copper complexes were observed to depend on the growth conditions of the GASH crystals. The data revealed the existence of two groups of Cu^{2+} complexes in GASH crystals grown at 40 °C, each group consisting of three physically equivalent but magnetically inequivalent Cu^{2+} complexes at the three substitutional Al^{3+} positions available for substitution by Cu^{2+} ions in the unit cell. The three magnetic axes of the Cu^{2+} complexes for one group were oriented symmetrically at about 7° from the crystalline c axis, while those of the other group were oriented symmetrically at about 60° from the c axis. In another GASH crystal grown at 70 °C, two different groups of Cu^{2+} complexes were detected with the three z axes of one group of Cu^{2+} complexes symmetrically oriented about the c axis and quite close to it, while those of the other group of Cu^{2+} ions were symmetrically oriented about the c axis at 110°. (The EPR results reported in the present paper correspond to those reported in [9] for the crystal grown at 40 °C.) It was concluded that the various Cu^{2+} complexes were located at tetragonally distorted octahedral symmetry sites. The Cu^{2+} spin-Hamiltonian parameters in GASH were not estimated rigorously, having been calculated from EPR line positions observed for the

orientation of the external magnetic field along only one or two directions. Further, the Jahn–Teller (JT) distortion was not detected because of lack of data over an extended temperature range.

The present paper reports a detailed variable-temperature X-band EPR study on a Cu^{2+}-doped GASH single crystal in the temperature range extending from liquid-helium temperature (3.9 K) to well above RT (433 K). A rigorous least-squares fitting procedure [10] has been used to estimate the spin-Hamiltonian parameters at various temperatures. Further, the EPR spectra below and above 423 K have been interpreted to indicate the occurrences of static and dynamic JT effects, respectively. Knowledge of the **g** principal values have been exploited to deduce the distortion of the $Cu(H_2O)_6^{2+}$ octahedra. The main features of the present study are described in the following sections.

2. Crystal structure and sample preparation

A GASH crystal possesses a hexagonal lattice structure [11–13] characterized by the space group $P31m$ (C_{3v}^2) with $Z = 3$; the unit-cell parameters are $a = 11.731$ Å and $c = 8.954$ Å [13]. The SO_4 tetrahedra are situated in a trigonal ordering perpendicular to the C_3 axis of the crystal. The Al atoms, lying on the C_3 symmetry axis, are surrounded by six water molecules, forming distorted $Al(H_2O)_6^{3+}$ octahedra. The guanidinium $[C(NH_2)_3]^+$ groups are situated below and above the $(H_2O)_6$ octahedra. Of the three Al^{3+} ions in the unit cell, two are equivalent to each other and belong to the so-called site II (point symmetry, C_3), while the third belongs to the so-called site I (point symmetry, C_{3v}).

Single crystals of Cu^{2+}-doped GASH were grown at RT (about 300 K) by slow evaporation of a saturated aqueous solution consisting of stoichiometric amounts of guanidinium and aluminium sulphate, to which was added a sufficient quantity of $CuSO_4 \cdot 5H_2O$ so that there were about ten Cu^{2+} ions for every 100 Al ions. (The resulting Cu^{2+} concentration in GASH crystals is usually much less than this, about 1%.) The solution was made slightly acidic with sulphuric acid to prevent hydrolysis. The slightly bluish transparent GASH crystals grew as hexagonal-shaped plates, whose normals were coincident with the crystal c axis.

The growth habit of GASH crystals is shown in figure 1, which exhibits the orientations of the crystal c axis, as well as the three magnetic axes and the average directions of the respective magnetic Z, X and Y axes of the three Cu^{2+} ions belonging to site II.

3. Experimental arrangement

EPR spectra were recorded on a Varian X-band V-4502 spectrometer connected to a Varian 12 in electromagnet driven by a Bruker power supply and controlled with a Bruker (BH-15) field controller. 100 kHz and 400 Hz field modulations were used above and below 123 K, respectively. The temperature was varied using a heater resistor inside a commercial liquid-helium cryostat with the use of a home-made cavity for measurements below 123 K. Temperatures in the range 123–420 K were maintained at the sample with a Varian variable-temperature controller unit (model E4540) attached to an Omega (model 870) microprocessor digital thermometer using a high-Q Varian cavity.
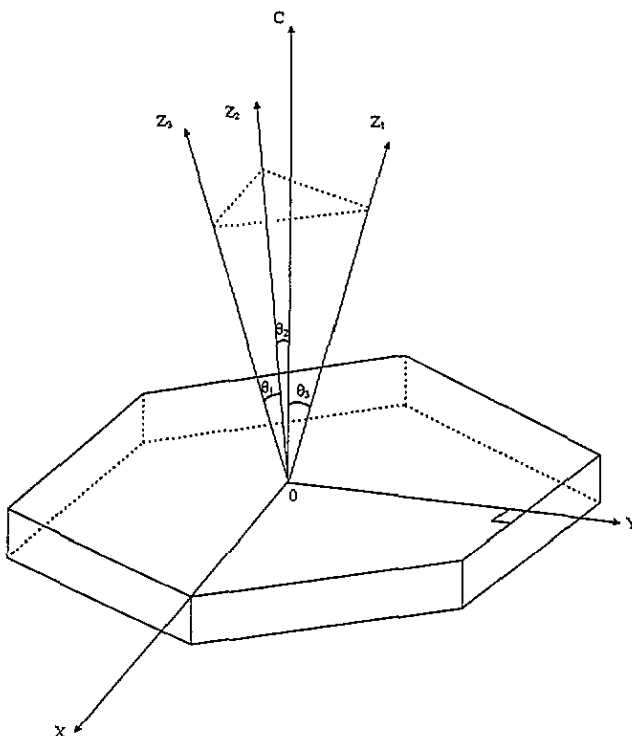
Figure 1. Growth habit of a GASH single crystal. The crystal c axis is perpendicular to the hexagonal face, while the three magnetic Z axes below 423 K for the ions belonging to site II are symmetrically located with respect to the c axis; the angles θ_1, θ_2 and θ_3 are equal to about 5–7°. The three magnetic X axes corresponding to site II lie close to each other and are oriented symmetrically about the line (OX) joining the centre of the hexagonal face to one of the corners of the face. In turn, the three magnetic Y axes lie very close to each other and are oriented symmetrically about the line (OY) passing through the centre of the face and perpendicular to one of the edges of the hexagonal face.

4. EPR spectra

4.1. Sites I and II

The EPR spectrum for a general orientation of the external magnetic field B exhibited two groups of lines, each group consisting of three sets of close-lying Cu^{2+} lines (quartets) belonging to three physically equivalent but magnetically inequivalent Cu(H$_2$O)$_6^{2+}$ complexes, corresponding to the so-called sites I and II. The intensities of the EPR lines due to Cu^{2+} ions at site II were about twice those at site I, because there are two ions at site II compared with one ion at site I in the unit cell of GASH. The orientations of the magnetic axes for the Cu^{2+} ions at sites I and II have been determined rather well by Sczaniecki [9], those for site II (see below) being in good agreement with the present determinations.

The lines for the Cu^{2+} ions situated at site I were difficult to identify for the orientation of B in the magnetic planes of Cu^{2+} ions at site II owing to their rather small intensities at various temperatures in comparison with those for the Cu^{2+} ions at site II. For this reason, the discussion will hereafter be confined to the EPR spectra observed for Cu^{2+} complexes belonging to site II, unless otherwise stated.

The EPR spectra were recorded for the orientation of B in two (at 293 and 373 K) or three (at 3.9, 82 and 123 K) magnetic planes (Z–X, X–Y or Z–Y) for Cu^{2+} ions belonging to site II at 5° intervals at every temperature chosen for measurement. The magnetic Z axes of the three magnetically inequivalent Cu^{2+} ions belonging to site II were found to be almost perpendicular to the hexagonal cleavage plane of the GASH crystal, being oriented symmetrically within 5–7° about the c axis. The corresponding three magnetic X axes were found to lie very close, within 5–7°, in a symmetrical manner, to the [1000] diagonal of the hexagonal face of the GASH crystal. Thus, the three magnetic Y axes lie very close (5–7°) to the direction perpendicular to the [1000] diagonal in the hexagonal face of the GASH crystal and oriented symmetrically about it. The orientations of the Z magnetic axes are exhibited in figure 1. The magnetic axes are defined to be such that the overall splitting of EPR lines exhibits extrema for B orientation parallel to them, these splittings successively decreasing for $B \| Z$ and $B \| X$, respectively. The overall splitting for $B \| Y$ is the same as that for $B \| X$ owing to axial symmetry. The orientations of the magnetic axes of the Cu^{2+} ions at the site II at present determined agree quite well with those determined by Sczaniecki [9].

4.2. *EPR spectra in the temperature interval 5–373 K*

The EPR spectra for Cu^{2+}-doped GASH in the 5–373 K range were not very different from each other except that the intensities of the EPR lines increased with decreasing temperature in this range, as seen from figure 2 which exhibits the EPR spectra for the $B \| c$ at 373, 293, 123 and 82 K. Typically, four hyperfine lines due to the interaction of the electronic and nuclear magnetic moments of the Cu^{2+} ion, representing total overlap of the three sets of spectra corresponding to the three $Cu(H_2O)_6^{2+}$ complexes belonging to site II for $B \| c$ were observed. These hyperfine lines were equispaced, indicating that the quadrupole interaction is negligible. Resolved splittings of the two outermost hyperfine lines due to the 30.91% abundant isotope $^{65}Cu^{2+}$ and 69.09% abundant isotope $^{63}Cu^{2+}$ were sometimes observed, but never in the case of the two middle lines, since the values of the nuclear magnetic moments of the ^{63}Cu and ^{65}Cu isotopes are about the same, being 2.2206 and 2.3789 nuclear magnetons, respectively [14]. At 123 K, three sets of spectra due to the three magnetically inequivalent Cu^{2+} belonging to site I are clearly seen positioned between the Cu^{2+} lines because the ions belong to site II and the DPPH line position. However, at higher temperatures the intensities of these lines belonging to site I were insufficient for them to be visible. From figure 2, it is seen that no phase transitions occur in the GASH crystal between 373 and 82 K, as deduced from the features of the EPR spectra. The Cu^{2+} spectrum for $B \| c$ at 123 K consisted of one set of four hyperfine lines because the Cu^{2+} ions substitute at site II and another set consisting of three groups of four hyperfine lines each belonging to site I, since the EPR spectra belonging to the three complexes for each set overlapped each other completely for $B \| c$.

From figure 3, which exhibits EPR spectra for several orientations of B in the Z–X plane at 123 K, it is seen that each of the four hyperfine lines of these two groups further splits into three close-lying lines, as the crystal was rotated so that B moved away from the c axis in the Z–X magnetic plane. This is because there exist three magnetically inequivalent but physically equivalent complexes with different orientations of their respective magnetic axes corresponding to the Cu^{2+} ions belonging to sites I and II.

The EPR spectra for the Cu^{2+} ions belonging to site II as recorded for various orientations of B in the magnetic Z–Y plane were found to be almost the same as those for the corresponding orientations of B in the magnetic Z–X plane at all temperatures. On the other hand, in the X–Y plane, which is perpendicular to the c axis, the EPR line positions for Cu^{2+} ions belonging to site II remained almost invariant with respect to the orientation
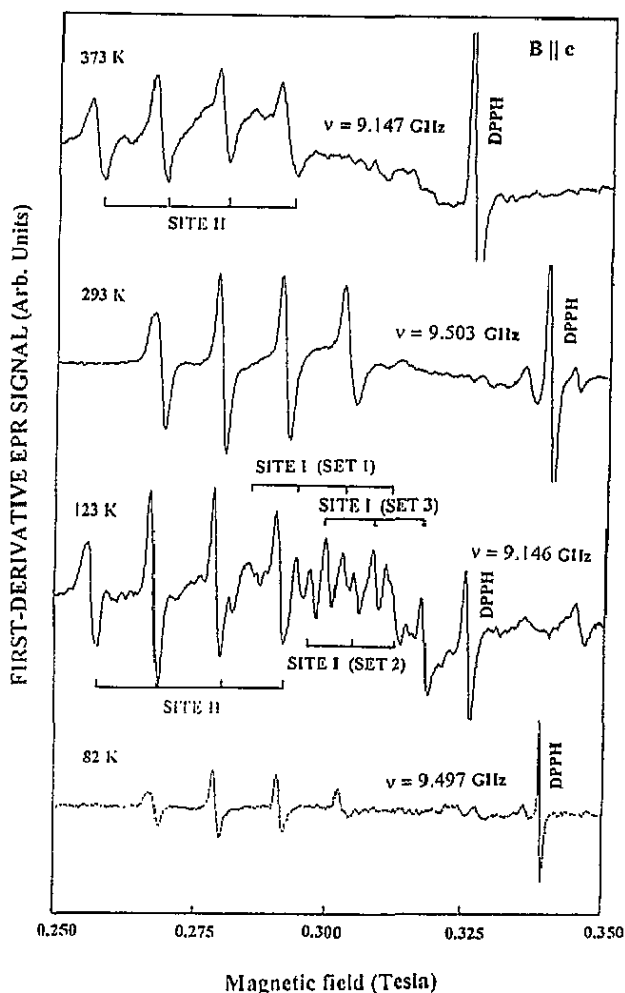
Figure 2. First-derivative X-band (about 9.2–9.5 GHz) EPR spectra of Cu^{2+}-doped GASH at 373, 293, 123 and 82 K for $B \| c$. The hyperfine lines due to Cu^{2+} ions at site II and those due to Cu^{2+} ions at site I have been indicated. The lines for the three magnetically inequivalent ions at site II while those for the three magnetically inequivalent ions at site I do not coincide for this orientation of B. Also, only three of the four hyperfine lines are clearly seen for two of the three magnetically inequivalent ions at site I.

of B, which demonstrates the axial site symmetry of the Cu^{2+} complexes belonging to site II about the c axis with a very slight splitting of each Cu^{2+} hyperfine line into three, indicating a slight deviation, about 5–7°, in a symmetrical manner of the magnetic Z axes of the three Cu^{2+} complexes from the c axis. Figure 4 exhibits the angular variation in the hyperfine-line positions of the various Cu^{2+} complexes belonging to site II in GASH for various orientations of B in the magnetic Z–X and Z–Y planes. It is seen from figure 4 that each hyperfine line lies at the minimum magnetic field value for $B \| Z$ (approximately c), while the corresponding maximum occurs at $B \| X (\equiv Y)$.
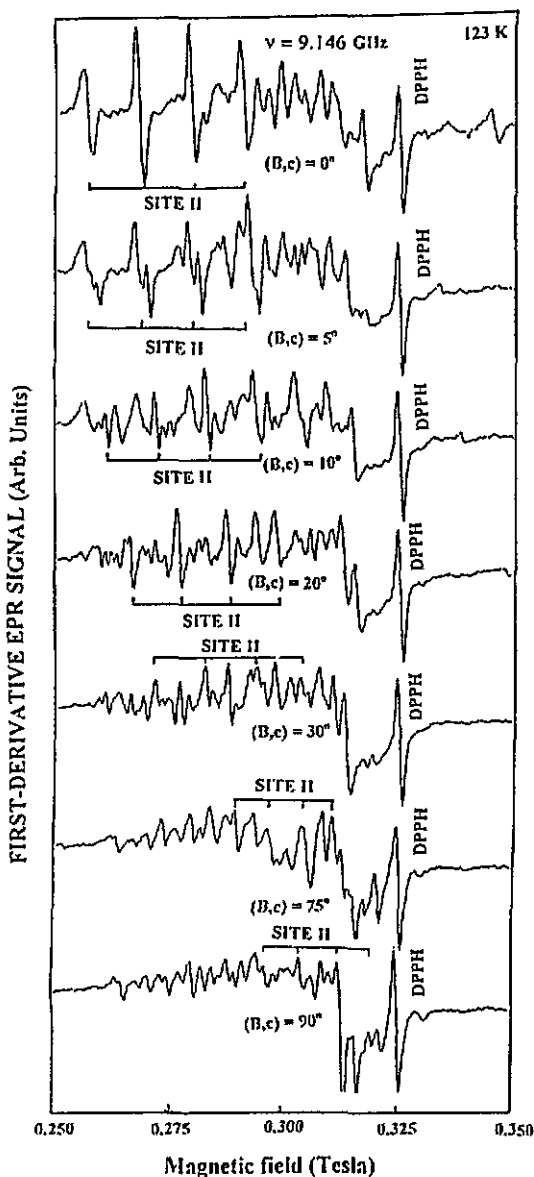
Figure 3. First-derivative X-band (about 9.2 GHz) EPR spectra of Cu^{2+}-doped GASH at 123 K for the orientation of the external magnetic field at 0°, 5°, 10°, 20°, 30°, 75° and 90° from the c axis in the plane passing through the c axis and the line (OX axis) connecting the centre of the hexagonal face and one of its corners. One set of hyperfine lines due to a magnetically inequivalent ion at site II has been indicated. (Those corresponding to the other two magnetically inequivalent ions at site II lie close by and can be identified by reference to figure 4.) The lines due to Cu^{2+} ions at site I have not been identified.

4.3. EPR spectra above 373 K: dynamic Jahn–Teller effect

Figure 5 shows the temperature variation in the EPR spectra over the range 373–433 K for the external magnetic field at 10° from the X axis in the X–Y plane. As the temperature was
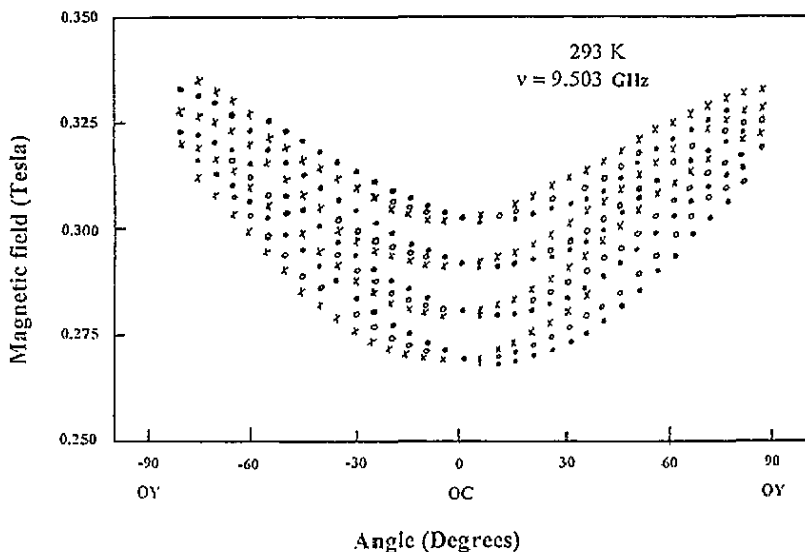
Figure 4. Angular variation in X-band (about 9.5 GHz) EPR line positions as observed for the orientation of the external magnetic field in the plane passing through the c axis and the line (OY axis) that passes through the centre of the hexagonal face and is perpendicular to one of its edges for Cu^{2+}-doped GASH at room temperature (293 K). Open circles, full circles and crosses represent line positions belonging to the same transition for the three magnetically inequivalent ions at site II. It is noted that some transitions are not clearly observed at all orientations of the external magnetic field.

increased above 373 K, the Cu^{2+} EPR spectra in GASH were observed to be similar to those at RT and at lower temperatures, except that the Cu^{2+} hyperfine lines became weaker and broader. The broadening of the lines is due to relaxation effects. Finally, at 423 K, only one single broad isotropic line, characterized by the value $g_{JT} = 2.17 = (g_\parallel + 2g_\perp)/3$, where $g_\parallel$ and $g_\perp$ are the principal values of the **g**-matrix at 373 K and lower temperatures as listed in table 1, was observed. This is similar to the case of Cu^{2+} in monopyrazine zinc sulphate trihydrate reported by Misra and Wang [15], where the single isotropic line occurred at 334 K as the temperature was increased. The position of the single broad line owing to the merger of the individual Cu^{2+} hyperfine lines with each other because the three Cu^{2+} complexes belong to site II moved to higher values of external magnetic field (i.e. to lower g-values), until it corresponded to the g-value $g_{JT} = (g_\parallel + 2g_\perp)/3$ as a result of the dynamic JT effect. This is easily understood by noting that the value of g_{JT} is doubly weighted in favour of $g_\perp$ and that $g_\perp < g_\parallel$. The appearance of only a single isotropic line is due to the manifestation of the type I dynamic JT effect [16] in GASH at temperatures above 423 K, explained to be due to motional averaging caused by rapid hopping between the equivalent JT-distorted Cu^{2+} sites (JT valleys), randomly distributed in the crystal with equal probabilities. This happens because the tetrahedrally elongated distortion of the $Cu^{2+}(H_2O)_6^{2+}$ octahedra in the present case is amenable to the JT effect [17–19]. This results in a time-averaged isotropic g-value [16], since the vibrational frequency (about 10^{13} Hz) is large compared with the frequency (about 10^{10} Hz) at which EPR is observed [15, 17]:

$$g_\parallel = g_\perp = g_e - 4\lambda/\Delta \simeq 2.2 \tag{1}$$

where g_e (= 2.0023) is the free-electron g-value, λ is the spin–orbit coupling constant for

free Cu^{2+} ions (equal to -830 cm^{-1} [17]), Δ ($= 10Dq \simeq 20|\lambda|$) is the octahedral crystal-field splitting for the Cu^{2+} ion. The isotropic value of $g \simeq 2.2$ is in agreement with that estimated using equation (1) and the $g_\parallel$ and the $g_\perp$ values listed in table 1 below 423 K (table 1).

Table 1. Principal values of the Cu^{2+} **g**- and **A**-matrices in GASH at site II. The principal axes of the **g**- and **A**-matrices are coincident with the magnetic Z and X, Y axes, respectively. The A-values represent the averages of those for the ^{63}Cu and ^{65}Cu isotopes due to the almost complete overlap of their spectra. n represents the number of lines simultaneously fitted to evaluate the parameters and MDL is the mean (percentage) deviation per line of the calculated energy difference of the pair of Cu^{2+} hyperfine energy levels participating in resonance from the klystron frequency. At 423 K the hyperfine splitting disappears and the **g**-tensor becomes isotropic because of the dynamic JT effect. It is noted for reference that the **g**- and **A**-values as estimated for Cu^{2+} ions at site I by Sczaniecki at RT are $g_\parallel = 2.422$, $g_\perp = 2.08$, $A_\parallel = 0.32$ GHz and $A_\perp = 0.09$ GHz. (No attempt has been made in the present paper to evaluate parameters for Cu^{2+} ions at site I.) The values for RT (last row) are those reported by Sczaniecki [9] for site II at RT.

T (K)	$g_\parallel$	$g_\perp$	$A_\parallel$ (GHz)	$A_\perp$ (GHz)	(MDL)	n
423	2.17(1)	2.17(1)				
373	2.371(5)	2.078(5)	0.386(5)	0.121(5)	0.11	140
293	2.373(5)	2.077(5)	0.382(5)	0.125(5)	0.07	140
123	2.377(5)	2.075(5)	0.375(5)	0.128(5)	0.15	140
82	2.381(5)	2.073(5)	0.369(5)	0.135(5)	0.16	140
3.9	2.38(5)	2.07(5)	0.37(5)	0.14(5)	0.2	140
RT	2.380	2.034	0.324	0.06		

4.4. Static Jahn–Taller effect below 423 K

When a Cu^{2+} ion substitutes for an Al^{3+} ion in GASH, the trigonally distorted octahedral symmetry of the $Al(H_2O)_6^{3+}$ complex changes to tetragonally elongated octahedral symmetry of the $Cu(H_2O)_6^{2+}$ complex (more details are given in section 6), because of its different size, ionized state and interaction with the water ligands from that of the Al^{3+} ion for which it substitutes. Moreover, as revealed from EPR spectra, the Cu^{2+} ions belonging to each of the sites I and II subdivide into three magnetically inequivalent but physically equivalent groups for a general orientation of B. This is due to the static JT effect [16–18] resulting in three orientations of the $Cu(H_2O)_6^{2+}$ complexes (JT valleys) associated with each of sites I and II, stabilized at their particular energies throughout the crystal [16, 17, 19].

The temperature-dependent **g**- and **A**-values for the Cu^{2+} ion at any site can be expressed, in general, as the averages over the three corresponding JT configurations, taking into account their Boltzmann populations determined by the energies of the JT valleys of $Cu(H_2O)_6^{2+}$ complexes and temperature [18]. In the present case, the values of $g_\parallel$, $g_\perp$, $A_\parallel$ and $A_\perp$ are found to be only weakly temperature dependent, implying that the energies of the three JT valleys lie very close to each other.

4.5. Alternative interpretation of static and dynamic Jahn–Teller effects

In sections 4.2 and 4.3 it was stated that a change from a static to a dynamic JT effect occurred as the temperature was increased above 423 K, as has been believed previously by JT researchers. However, the current view of many JT specialists, including Ham himself, is
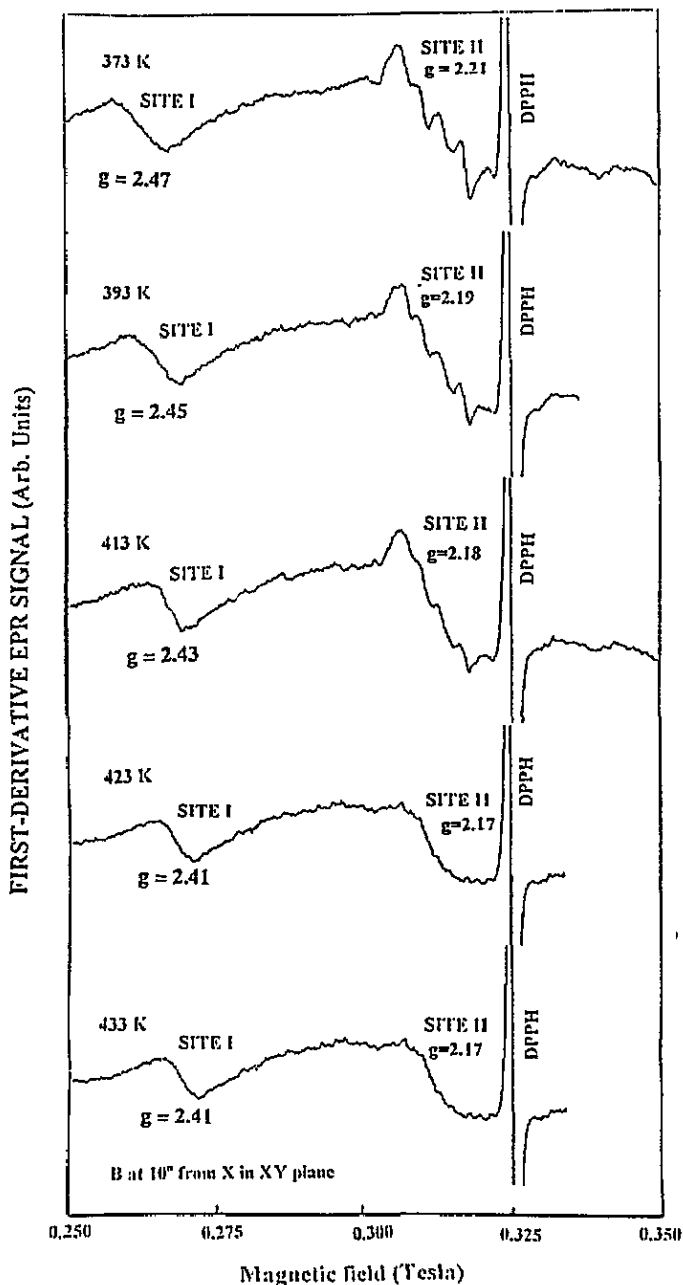
Figure 5. First-derivative X-band (about 9.5 GHz) EPR spectra of Cu^{2+}-doped GASH for the external magnetic field orientation at 10° from the OX axis (as defined in the caption for figure 1) in the (approximate) X–Y plane (coincident with the hexagonal face of the crystal) at 373, 393, 413, 423 and 433 K. The g-values at the centre of the various hyperfine Cu^{2+} quartets have been indicated for Cu^{2+} ions situated at sites I and II.

that it is physically incorrect to talk about the static JT effect [20, 21]. Even at extremely low temperatures, there is tunnelling between different so-called static configurations, resulting

in a dynamic JT effect. Another way of understanding this is to argue that the Hamiltonian, and hence the wavefunctions, must reflect the true symmetry of the crystal, which is higher than that of a static configuration. The potential energy surface of a JT system contains various minima or 'wells' in the coordinate (Q-) space, several of which are absolute energy minima, each one of which corresponds to a static JT distortion. In a pure JT situation, there is tunnelling through each well, resulting in a dynamic situation. However, in a real crystal, there will be imperfections present, introducing local strain among other things. The effect of any one strain will be to lower the energy of some (one) wells with respect to the others. Tunnelling can no longer occur between all minima as before, and it appears that a static JT effect is present. The net effect of all strains is to allow all static configurations.

The temperature effects observed can be explained as follows. The full potential-energy surface consists of parabolic-like minima which intersect at higher energies. As the temperature is increased, higher excited states in the potential wells are occupied, and tunnelling between the states occurs even though the minima of the wells have different energies from each other.

4.6. Linewidths

The average linewidth of the hyperfine lines, 20 ± 5 G, remained the same at temperatures below 373 K and, was independent of the orientation and intensity of the external magnetic field. This implies that the spin–lattice relaxation time of the Cu^{2+} ion in GASH does not change appreciably below 373 K, presumably owing to the absence of host paramagnetic ions in GASH [22].

5. Spin Hamiltonian and evaluation of parameters

The EPR line positions of the Cu^{2+} ion in GASH were fitted to the following spin Hamiltonian, omitting the nuclear Zeeman term since its effect cannot be seen in the EPR spectra, and taking into account the axial site symmetry [9]:

$$\mathcal{H} = \mu_B g_\parallel B_z S_z + \mu_B g_\perp (B_x S_x + B_y S_y) + A_\parallel S_z I_z + A_\perp (S_x I_x + S_y I_y) \qquad (2)$$

where μ_B is the Bohr magneton, $g_\parallel$ and $g_\perp$ are the principal values of the **g**-matrix, $A_\parallel$ and $A_\perp$ are the principal values of the hyperfine **A**-matrix, and $S(= \frac{1}{2})$ and $I(= \frac{3}{2}$ for both ^{63}Cu and ^{65}Cu isotopes) are the electronic and nuclear spins, respectively, of the Cu^{2+} ion. The least-squares fitting technique used for the evaluation of spin-Hamiltonian parameters ($g_\parallel$, $g_\perp$, A and $A_\perp$), using eigenvalues calculated to second order in perturbation, and fitting simultaneously all the line positions recorded for the orientation of the external magnetic field in the various magnetic planes, has been described in detail by Misra [10]. The values of the parameters so evaluated are listed in table 1. The **g**- and **A**-principal values are expected to be the same for the three magnetically inequivalent ions belonging to site II, since they are physically equivalent to each other.

6. Electronic ground state of the Cu^{2+} ion in GASH

The ground state of the Cu^{2+} ion in GASH is deduced to be $^2B_{1g}$ ($|X^2 - Y^2\rangle$), characteristic of octahedral symmetry distorted by tetragonal elongation, by examination of the $g_\parallel$ and $g_\perp$-values as follows. For tetragonal elongation of the $Cu(H_2O)_6^{2+}$ complex, the energy

level sequence, in increasing order of energy, is $^2B_{1g}$ ($|X^2 - Y^2\rangle$) (ground state), $^2A_{1g}$ ($|3Z^2 - R^2\rangle$), $^2B_{2g}$ ($|XY\rangle$) and ^2E_g ($|XZ\rangle$, $|YZ\rangle$) [17, 19]. The ground-state g-values are given by

$$g_\| = g_e - \frac{8\lambda}{\Delta E_{xy}} \qquad g_\perp = g_e - \frac{2\lambda}{\Delta E_{xz,yz}} \tag{3}$$

where ΔE_{xy} and $\Delta E_{xz,yz}$ are the energies of the singlet state $|XY\rangle$ and doubly degenerate states $|XZ\rangle$ and $|YZ\rangle$, respectively, relative to the energy of the ground state $|X^2 - Y^2\rangle$. Since the spin–orbit coupling constant λ is negative for the Cu²⁺ ion (d⁹ configuration) according to Hund's rule [17], $g_\| > g_\perp > 2.0023$ from equation (3). Further, the energy denominators in equation (3) are about 20 times the magnitude of λ [17]; the g-factors for Cu²⁺ in GASH for tetragonal elongation [17, 19] are expected to be $g_\| \simeq 2.4$ and $g_\perp \simeq 2.1$, consistent with the values estimated (table 1). That the ground state is $|X^2 - Y^2\rangle$ is further supported by the criterion given by Budley and Hathaway [23] wherein, if the value of $R = (g_1 - g_2)/(g_3 - g_1)$ is less than unity, a predominantly $|X^2 - Y^2\rangle$ ground state is expected. In the present case, $g_\| = g_3 > g_\perp = g_1 = g_2$, yielding $R = 0$. (It is noted that, had there been tetragonal compression of the $Cu(H_2O)_6^{2+}$ complex, the $|3Z^2 - R^2\rangle$ state would have been the ground state characterized by $g_\perp > g_\| \cong 2.0023$ [17, 19, 24].)

7. Concluding remarks

The main features of the EPR study presented in this paper on a Cu²⁺-doped GASH single crystal, in the temperature range 5–433 K, are as follows.

(i) There exist two types of Cu²⁺ complex belonging to the two so-called sites I and II. Three slightly magnetically inequivalent but physically inequivalent Cu²⁺ ions belong to each site below 423 K. The orientations of the three sets of magnetic axes of the Cu²⁺ ions belonging to site II have been determined. This information, in conjunction with the results of Sczaniecki [9] for the orientation of magnetic axes corresponding to three Cu²⁺ ions at site I, and also those in another crystal grown at 70 °C, can be considered to be complete in so far as the orientations of the magnetic axes of the various possible Cu²⁺ complexes that can be formed in GASH are concerned.

(ii) The orientations and principal values of the **g**- and **A**-matrices for the Cu²⁺ ions in GASH, occupying site II, have been estimated using a rigorous least-squares fitting procedure at 3.9, 82, 123, 293 and 373 K.

(iii) The dynamic JT effect has been observed to occur at temperatures above 423 K, while below this temperature the static JT effect prevails, resulting in three groups of physically equivalent but magnetically inequivalent $Cu(H_2O)_6^{2+}$ complexes belonging to each of the sites I and II.

(iv) The symmetry of the $Cu(H_2O)_6^{2+}$ complexes in GASH has been deducted from the observed g-values to be tetragonally elongated octahedral. The ground state of the Cu²⁺ ion in GASH is, thus, the orbital singlet state $|X^2 - Y^2\rangle$.

(v) Below 373 K, the Cu²⁺ EPR linewidths are found to be almost independent of the temperature, as well as of the orientation and intensity of the external Zeeman field, within experimental error.

Acknowledgments

References

[1]   Holden A N, Matthias B T, Merz W J and Remeika J P 1955 *Phys. Rev.* **98** 546
[2]   Holden A N, Merz W J, Mathias B T and Remeika J P 1956 *Phys. Rev.* **101** 962
[3]   Daniels J M and Wesemeyer H 1958 *Can. J. Phys.* **36** 144
[4]   Schwartz R W and Carlin R L 1970 *J. Am. Chem. Soc.* **92** 6763
[5]   Misra S K, Giguère P and Sharp G R 1977 *J. Chem. Phys.* **66** 1758
[6]   Brock E G, Stripe D and Hormates E I 1962 *J. Chem. Phys.* **37** 2735
[7]   Misra S K and Sharp G R 1976 *J. Chem. Phys.* **65** 3605
[8]   Milsch B and Windsch W 1978 *Phys. Status Solidi* b **89** 241
[9]   Sczaniecki B 1970 *Acta Phys. Pol.* A **38** 189
[10] Misra S K 1984 *Physica* B **124** 53
[11] Geller S and Booth D P 1958 *Z. Kristallogr.* **111** 2
[12] Schein B J B, Lingafelter E C and Stewart J M 1967 *J. Chem. Phys.* **47** 5183
[13] Nikolic P M, Roys W B, Maricic X, Gledhill G A, Duric S, Radukic G, Radišic V, Milhajlovic P, Todorovic D M and Vasiljevic D 1993 *J. Phys.: Condens. Matter* **5** 3039
[14] Andrew E R 1969 *Nuclear Magnetic Resonance* (Cambridge: Cambridge University Press)
[15] Misra S K and Wang C 1989 *J. Phys.: Condens. Matter* **1** 771
[16] Ham F S 1972 *Electron Paramagnetic Resonance* ed S Geschwind (New York: Plenum) p 54
[17] Abragam A and Bleaney B 1970 *Electron Paramagnetic Resonance of Transition Ions* (Oxford: Clarendon)
[18] Petrashen V E, Yablokov Yu V and Davidovich R L 1980 *Phys. Status Solidi* b **101** 117
[19] Vassilikon-Dava A B and Lehmann G 1987 *Fortschr. Miner.* **65** 173 (It should be noted that the energy-level sequence given in figure 1 of this reference applies to a d^1 ion (with the positive absolute sign of the spin–orbit coupling constant); for a d^9 ion, such as Cu^{2+} with the negative absolute sign for λ, the energy level sequence should be reversed in order to conform to that described in the present paper)
[20] Dunn J L and Bates C A 1988 *J. Phys. C: Solid State Phys.* **21** 2495
[21] Dunn J L 1995 Private communication
[22] Misra S K 1987 *Magn. Reson. Rev.* **12** 191
[23] Budley R J and Hathaway B J 1970 *J. Chem. Soc.* A 2799
[24] Pilbrow J R 1990 *Transition Ion Electron Paramagnetic Resonance* (Oxford: Clarendon)